21st INTELEC, June 6–9, 1999, Copenhagen, Denmark

A New Switching Loss Reduced Discontinuous PWM Scheme for a Unidirectional Three-Phase/Switch/Level Boost-Type PWM (VIENNA) Rectifier

Johann W. KOLAR and Uwe DROFENIK

Technical University Vienna
Dept. of Electrical Drives and Machines
Gusshausstrasse 27/E372, Vienna A-1040
AUSTRIA/Europe
Tel.: +43-1-58801-37225 Fax.: +43-1-58801-37299
e-mail: hkolar@ieam.tuwien.ac.at

Abstract. In this paper the applicability of discontinuous modulation for a three-phase/switch/level PWM rectifier system is investigated. As an analysis of the voltage formation of the system shows, the clamping in intervals (in each case, of one bridge leg to one bus of the DC output circuit) being characteristic for discontinuous modulation can occur in regions lying symmetrically around the maxima of the related phase currents. This results in a maximum reduction of the switching power loss. The increase of the effective pulse frequency (as compared to continuous modulation for equal switching losses) made possible thereby is calculated analytically. Furthermore, by digital simulation the rms value of the mains current harmonics resulting for discontinuous modulation and increased pulse frequency is determined in dependency on the modulation depth. Also, it is compared to the harmonic characteristic for harmonic optimal continuous modulation. The load on the power semiconductors and on the output capacitors (characterized by the rms value and the amplitude of the low-frequency harmonics of the capacitor current) is included into the comparison of the modulation methods. Finally, the time shape of the phase modulation functions (to be provided for the control of the voltage formation of the system based on a subharmonic oscillation method) for discontinuous modulation is calculated and the control of the potential of the output voltage center point is discussed.

1 Introduction

Three-phase boost-type DC voltage link PWM rectifier systems (cf. e.g. p. 244 in [1]) have in general no connection between the star point of the supplying mains and the center point of the output DC voltage. Therefore, only the differences of the phase voltages formed at the input of the system have influence (in connection with the mains voltage) on the formation of the fundamentals of the mains phase currents. Therefore, a sinusoidal guidance of the mains phase currents can be realized by pulsing of only two bridge legs in each case; the third bridge leg (which changes in cyclic manner between the phases within the mains period) is clamped to a bus of the output circuit. This form of voltage control which has been proposed initially in [2] for two-level inverters is called discontinuous modulation [3].

By the clamping of a phase in time intervals (*discontinuous* modulation) the switching losses are reduced as compared to using constant switching frequency of the bridge (*continuous* modulation). For a defined value of the switching loss this allows an increase of the effective pulse frequency. This leads to a significant reduction of the rms value of the mains current harmonics for high values of the modulation depth, as shown for two-level PWM rectifiers in [3]. Furthermore, by this method the harmonic components of the mains current which are grouped around multiples of the pulse frequency are shifted to higher frequencies. This allows to reduce the filtering effort being required for the suppression of conducted EMI; also, the power density of the converter system is increased.

Based on the advantages of discontinuous modulation as known for two-level converters and how discussed previously, in this paper the question is analyzed whether this modulation method can also be applied to the control of a new unidirectional three-phase/switch/level PWM rectifier (cf. **Fig.1**) as presented in [4]. The other question analyzed is to what extent the operational behavior is improved as compared to continuous modulation. For the investigations we assume resistive fundamental mains behavior, constant output voltage and symmetry of the output partial voltages.

As is immediately clear from the circuit structure, the formation of the input phase voltages of the system depicted in Fig.1 is influenced also by the signs of the phase currents besides the switching states of the power transistors. As shown in **section 2** of the final paper, despite this limitation of the controllability of the input voltage formation of the sytem one can achieve a clamping of one bridge leg in each case in regions which lie symmetrically around the maxima and zero crossings of the related phase currents. There, the allowable widths of the clamping intervals is determined by the value of the modulation depth. The resulting dependency of the admissible increase (for equal switching losses as compared to continuous modulation) of the effective pulse frequency on the modulation depth is calculated analytically in **section 3**. In **section 4**, the rms value of the mains current harmonics resulting for discontinuous modulation is determined in dependency on the modulation depth by analytical calculation and digital simulation. The comparison with harmonic-optimal continuous modulation makes clear that for the considered three-level PWM rectifier system the discontinuous modulation leads (similarly to two-level converters) for high modulation depth to a significantly reduced rms value of the mains current harmonics. Furthermore, for both modulation methods the load on the output capacitors (rms value and low-frequency harmonics of the capacitor currents) are compared (cf. **section 5**). In **section 6**, the time shape of the phase modulation functions to be provided for discontinuous modulation for control of the voltage formation

0-7803-5624-1/99/$10.00 © 1999 IEEE

of the system based on a subharmonic oscillation method is given. Finally, in **section 7**, the inclusion of a control of the potential of the output voltage center point into the voltage control is discussed.

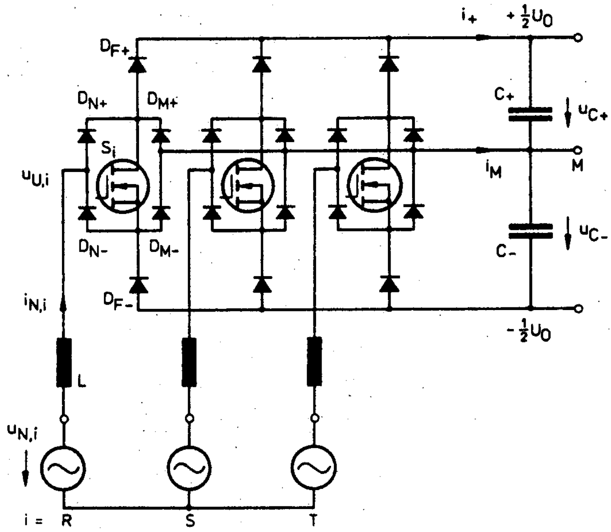

Fig.1: Basic structure of the power circuit of an unidirectional three-phase/switch/level PWM (VIENNA) rectifier as proposed in [4]. Concerning the basic function this circuit is comparable to a concept proposed in [6] which, however, employs two power switches in each bridge leg. For applying the control concept proposed in this paper to this circuit both transistors of a bridge leg have to be controlled by the gate signal of the corresponding single switch of the VIENNA Rectifier.

2 Basic Considerations

Before analyzing the discontinuous modulation scheme in detail we want to briefly summarize the basics of the control of the VIENNA Rectifier in the following. Furthermore, in section 2.2 the procedure for a digital simulation of the system is discussed.

2.1 Control of the Rectifier Input Voltage, Space Vector Modulation

With the assumption of a sinusoidal, symmetrical mains voltage system according to a space vector

$$\underline{u}_N = \hat{U}_N \exp j\varphi_N \qquad \varphi_N = \omega_N t\ , \tag{1}$$

at the input of the rectifier system in the average over a pulse periode T_P a voltage space vector

$$\underline{u}_U^* = \hat{U}_U^* \exp j\varphi_U = \hat{U}_N \exp j\varphi_N - j\,\omega_N L\,\underline{i}_N \tag{2}$$

has to be formed in order to obtain an ideally sinusoidal shape of the mains current

$$\underline{i}_N^* = \hat{I}_N^* \exp j\varphi_N\ . \tag{3}$$

to be provided. The voltage space vectors $\underline{u}_U^* = \underline{u}_{U,(1)}$ and $\underline{i}_N^* = \underline{i}_{N,(1)}$ describe the fundamental contributions $u_{U,i,(1)}$ (with amplitude $\hat{U}_{U,(1)} = \hat{U}_U^*$) and/or $i_{N,i,(1)}$ (with amplitude $\hat{I}_{N,(1)} = \hat{I}_N^*$) of the phase quantities $u_{U,i}$ and/or $i_{N,i}$ ($i = R, S, T$). In case of high switching frequency and/or low inductance of the input inductors L_N due to the geometric addition of mains voltage and voltage loss of the inductances L_N we can have in good approximation

$$\hat{U}_U^* \approx \hat{U}_N\ ; \tag{4}$$

for stationary operation the amplitude of the ideal value of the input voltage $\hat{U}_U^*$ is basically defined via the amplitude of the mains voltage. The amplitude $\hat{U}_U^*$ is characterized by the modulation index of the system

$$M = \frac{\hat{U}_U^*}{\frac{1}{2}U_O}\ . \tag{5}$$

The limit to overmodulation is reached for

$$M_{\max} = \frac{2}{\sqrt{3}} \qquad (\hat{U}_U^* = \frac{U_O}{\sqrt{3}}) \tag{6}$$

In this paper only the interval $M \in [\frac{2}{3}, \frac{2}{\sqrt{3}}]$, which is of special interest for a practical realization, will be investigated. Because of the limited blocking voltage stress on the power semiconductors and/or because of the relatively high on-resistance and switching-losses of switching devices of high blocking voltage, in general a low value of the output voltage U_O (referring to the minimum voltage $U_{O,\min} \approx \sqrt{3}\hat{U}_N$, Eq.(4) and Eq.(5)) is set and/or the system is operated close to the overmodulation limit $M_{\max}$.

The space vectors being available for generating the vector $\underline{u}_U^*$ and their correspondence to the switching states of the system (denoted by the triple of quantities (s_R, s_S, s_T) formed by the phase switching functions s_j) are determined according to

$$u_{U,i} = \begin{cases} \text{sign}\{i_{N,i}\}\frac{U_O}{2} & \text{if} \quad s_i = 0 \\ 0 & \text{if} \quad s_i = 1 \end{cases} \tag{7}$$

by the signs of the phase currents $i_{N,i}$ and/or by the angular position of the current space vector $\underline{i}_N$ [7]. Basically we have at our disposal for the approximation of the continuous motion of $\underline{u}_{U,(1)}$ for each combination of signs of the three-phase currents only 8 different voltage space vectors. The voltage space vectors for $\varphi_N \in (-\frac{\pi}{6}, +\frac{\pi}{6})$ ($i_{N,R} > 0, i_{N,S} < 0, i_{N,T} < 0$) are shown in **Fig.2**. The vector $\underline{u}_U^*$ therefore can be formed only in the average over a pulse half period $\frac{1}{2}T_P$. With regard to a best possible approximation one applies only those rectifier voltage space vectors $\underline{u}_{U,j}$ lying in the immediate vicinity of the reference vector tip or those switching states j which are assigned to the corner points of that triangular region of the space vector plane into which the tip of the vector $\underline{u}_U^*$ points. Accordingly, there follows for the conditions of Fig.2 ($j = (000), (010), (011), (100)$)

$$\begin{aligned} \underline{u}_U^* = \; & \delta_{(100)}\underline{u}_{U,(100)} + \delta_{(000)}\underline{u}_{U,(000)} + \\ & + \delta_{(010)}\underline{u}_{U,(010)} + \delta_{(011)}\underline{u}_{U,(011)}\ . \end{aligned} \tag{8}$$

In order to minimize the switching frequency of the system we now arrange the switching states within each pulse half period in such a way that the subsequent state can always be obtained by switching of only one bridge leg. If we select arbitrarily (100) as initial switching state there results within each pulse period T_P a switching state sequence

$$\begin{aligned} & \ldots|_{t_\mu=0}(100) - (000) - (010) - (011)|_{t_\mu=\frac{1}{2}T_P} \\ & (011) - (010) - (000) - (100)|_{t_\mu=T_P} \cdots \end{aligned} \tag{9}$$

(if sector I in Fig.2 is used as basis); due to the requirement of a minimum number of switchings one has to reverse the sequence of the voltage space vectors $\underline{u}_{U,i}$ after each pulse half period.

The relative on-time δ_j of the switching states $j = (000)$ and (010) now can be calculated directly via evaluation of simple geometric relations [8]. The sum of the relative on-time of the switching states (100) and (011) is calculated via

$$\delta_{(100)} + \delta_{(011)} = 1 - \delta_{(000)} - \delta_{(010)} \tag{10}$$

because both switching states (100) and (011) result in the same voltage space vector $\underline{u}_{U,(100)} = \underline{u}_{U,(011)}$ for a realtion of the pahse currents $i_{N,R} > 0, i_{N,S} < 0, i_{N,T} > 0$ and symmetry $U_{C+} = U_{C-} = \frac{U_O}{2}$ of the output partial voltages (cf. Fig.2 and Fig.7 in [9]).

As a more detailed analysis shows for every combination of the signs of the input phase currents there is a redundancy of always two switching states according to the forming of the input voltages of the system. The distribution of the redundant voltage vectors between begin and end of each pulse half period constitutes a degree of freedom of the voltage control, therefore.

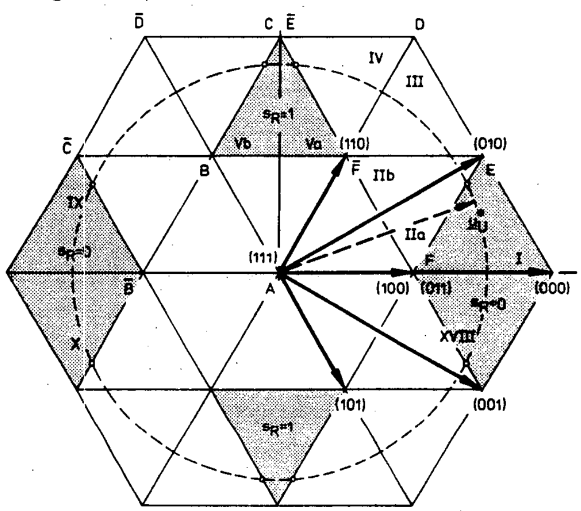

Fig.2: Voltage space vectors $\underline{u}_{U,j}$ of the rectifier input phase voltages $u_{U,j}$ for $i_{N,R} > 0, i_{N,S} > 0, i_{N,T} < 0$. For $i_{N,R}, i_{N,S} > 0, i_{N,T} < 0$ the voltage space vectors of the rectifier are rotated counter-clockwise by $\frac{\pi}{3}$ (cf. hexagon A-B-C-D-E-F); for $i_{N,R} < 0, i_{N,S} > 0, i_{N,T} < 0$ the corresonding hexagon is defined by corner points $A - \bar{B} - \bar{C} - \bar{D} - C - \bar{F}$. Those sectors, where in case of discontinuous modulation **(a)** phase R is clamped are marked with dots (in sectors I, IX, X, etc. the power transistor T_R remains in the off-state, in sectors V and XIV T_R is always on). $\underline{u}_U^*$ denotes the reference value of the rectifier input voltage for stationary operation.

Redundant switching states result in center point currents i_M of same value but different sign (cf. Tab.1 in [9]). Therefore, this degree of freedom can be used, e.g. for conrolling the neutral point potential u_M of the neutral point (output voltage center point) M . For a clear representation again the conditions given for $\varphi_N \in (-\frac{\pi}{6}, +\frac{\pi}{6})$ will be studied. For the center point current we have in general

$$i_M = s_R\, i_{N,R} + s_S\, i_{N,S} + s_T\, i_{N,T}\,. \tag{11}$$

Based on Eq.(11) the center point current corresponding to the redundant switching states (100) and (011) is calculated as

$$i_M = \begin{cases} -i_{N,R} & \text{for } (011) \\ +i_{N,R} & \text{for } (100) \end{cases} . \tag{12}$$

Therefore, for the local average value of the center point current being related to a pulse half periode there follows

$$i_{M,\mathrm{avg}} = \delta_{(010)}\, i_{N,S} - [\delta_{(011)} - \delta_{(100)}]\, i_{N,R}\,. \tag{13}$$

The distribution of the overall on-time between the redundant switching states (100) and (011) has essential influence on the local average value $i_{M,\mathrm{avg}}$ of the center point current and can, therefore, be used for controlling the neutral point potential and/or the symmetry of the partial output voltages u_{C+} and u_{C-}. In the following this distribution shall be denoted by

$$\rho_{--} = \frac{\delta_{--}}{\delta_{++} + \delta_{--}} \qquad \rho_{--} \in [0, 1]\,. \tag{14}$$

There, δ_{++} denotes the relative on-time of the respective redundant switching state (giving a positive center point current contribution) and δ_{--} denotes the relative on-time of the inverse redundant switching state (giving a negative center point current contribution). For $\varphi_N \in (-\frac{\pi}{6}, +\frac{\pi}{6})$ we have, therefore, the relationships $\delta_{++} = \delta_{(100)}$ and $\delta_{--} = \delta_{(011)}$. A symmetric distribution of the redundant switching states between begin and end of each pulse half period is given, therefore, for $\rho_{--} = 0.5$.

2.2 Analysis of the System Operating Behaviour by Digital Simulation, Normalization

For analyzing the system behaviour in this paper direct analytical calculations and/or digital simulations are performed. For the simulation parameters we select rated quantities which are characteristic for an application of the system in the European low voltage mains (e.g., for application as input stage of an uninterruptable power supply (UPS), cf. section 3 in [11])

$$\begin{aligned} U_{N,\mathrm{rms}} &= 230\,\mathrm{V} \\ U_O &= 700\,\mathrm{V} \\ \hat{I}_N^* &= 18\,\mathrm{A} \\ f_P &= 16\,\mathrm{kHz} \\ L &= 1\,\mathrm{mH}\,. \end{aligned}$$

The relatively low value of the (constant) converter switching frequency $f_P = 16\,\mathrm{kHz}$ is set with respect to a short simulation time. A change of the modulation index (rated value $M = 0.93$) is obtained for constant output voltage U_O via changing the mains voltage amplitude $\hat{U}_N$. In order to limit the considerations to the essentials we assume U_O to be impressed. This makes possible to avoid the design and simulation of the output voltage control loop. The guidance of the mains phase currents is realized by setting the space vector $\underline{u}_U^*$ (cf. Eq.(2)) which is present in the average over a pulse half period in such a way that the mains current space vector $\underline{i}_N$ is transferred from one point in the reference value circle $\underline{i}_N^*$ into a position associated to a time difference $\frac{1}{2}T_P$. One also can say that the tip of the current space vector is moved (as seen in time average) along the reference value circle. This circle is defined by the fundamentals of the mains phase currents. By application of this predictive current control method and/or a deadbeat principle we can avoid the time-consuming simulation of the current control initial transient and/or can simulate the stationary operating behaviour directly.

sector	$(s_R, s_S, s_T)_{\text{red}}$	mod. method (a)	mod. method (b)	$\rho_{--,(a)}$	$\rho_{--,(b)}$
I	(100), (011)	$\ldots(\underline{0}11)\text{-}(\underline{0}10)\text{-}(\underline{0}00)\ldots$	$\ldots(10\underline{0})\text{-}(00\underline{0})\text{-}(01\underline{0})\ldots$	1	0
IIa	(100), (011)	$\ldots(0\underline{1}1)\text{-}(0\underline{1}0)\text{-}(1\underline{1}0)\ldots$	$\ldots(10\underline{0})\text{-}(11\underline{0})\text{-}(01\underline{0})\ldots$	1	0
IIb	(110), (001)	$\ldots(1\underline{1}0)\text{-}(0\underline{1}0)\text{-}(0\underline{1}1)\ldots$	$\ldots(\underline{0}01)\text{-}(\underline{0}11)\text{-}(\underline{0}10)\ldots$	0	1
III	(110), (001)	$\ldots(11\underline{0})\text{-}(01\underline{0})\text{-}(00\underline{0})\ldots$	$\ldots(\underline{0}01)\text{-}(\underline{0}00)\text{-}(\underline{0}10)\ldots$	0	1
IV	(110), (001)	$\ldots(11\underline{0})\text{-}(10\underline{0})\text{-}(00\underline{0})\ldots$	$\ldots(0\underline{0}1)\text{-}(0\underline{0}0)\text{-}(1\underline{0}0)\ldots$	0	1
Va	(110), (001)	$\ldots(\underline{1}10)\text{-}(\underline{1}00)\text{-}(\underline{1}01)\ldots$	$\ldots(0\underline{0}1)\text{-}(1\underline{0}1)\text{-}(1\underline{0}0)\ldots$	0	1
Vb	(101), (010)	$\ldots(\underline{1}01)\text{-}(\underline{1}00)\text{-}(\underline{1}10)\ldots$	$\ldots(01\underline{0})\text{-}(11\underline{0})\text{-}(10\underline{0})\ldots$	1	0
VI	(101), (010)	$\ldots(1\underline{0}1)\text{-}(1\underline{0}0)\text{-}(0\underline{0}0)\ldots$	$\ldots(01\underline{0})\text{-}(00\underline{0})\text{-}(10\underline{0})\ldots$	1	0

Tab.1: Switching state sequences within one pulse period and value of the control parameter ρ_{--} for discontinuous modulation (a) and discontinuous modulation (b) of a three-phase/switch/level (VIENNA) PWM rectifier. The denomination of the sectors is related to the space vector plane in Fig.2. $(s_R, s_S, s_T)_{\text{red}}$ describes the redundant switching states that are dependent on the combination of signs of the mains phase currents.

2.2.1 Normalization

In order to gain a far-reaching independency of the simulation results of the selected specific simulation parameters (and/or to gain results which are not limited to specific operating parameters and device characteristics) the calculated average and rms current values are related to the peak value $\hat{I}_N^*$ of the mains current reference value and/or the mains phase current fundamental $\hat{I}_{N,(1)} = \hat{I}_N^*$; for the normalized rms value of the power transistor current we have then, e.g.,

$$I_{T,\text{rms,r}} = \frac{1}{\hat{I}_{N,(1)}} I_{T,\text{rms}} \,. \tag{15}$$

The normalization basis of the rms value of the mains current harmonics $\Delta I_{N,\text{rms}}$ is set to

$$\Delta I_{\text{r}} = \frac{U_O T_P}{8L} \,. \tag{16}$$

Then,

$$\Delta I_{N,\text{rms,r}} = \frac{1}{\Delta I_{\text{r}}} \Delta I_{N,\text{rms}} \tag{17}$$

represents a characteristic value which is independent of $f_P = T_P^{-1}$ and L in a first approximation.

3 Discontinuous Modulation

As described in section 2.1 the voltage formed in the average over a pulse half period is not influenced by the control parameter $\rho_{--} \in [0,1]$. If now $\rho_{--} = 1$ is set in sector I of the space vector plane (cf. Fig.2) there results a switching state sequence

$$\begin{aligned} \cdots|_{t_\mu=0}(\underline{0}11) - (\underline{0}10) - (\underline{0}00)|_{t_\mu=\frac{1}{2}T_P} \\ (\underline{0}00) - (\underline{0}10) - (\underline{0}11)|_{t_\mu=T_P} \cdots \end{aligned} \tag{18}$$

where the power transistor T_R of bridge leg R remains in the off-state ($s_R = 0$). This is the motivation for posing the general question (which will be investigated in detail in the following) to what extent the choice of $\rho_{--} = 1$ or 0 within sectors of the mains period can reduce the switching losses of each phase. A main advantage of reducing the switching losses as compared to continuous switching of all phases is the possibility of operating the system at higher effective switching frequency for equal thermal stress of the power transistors. This increase of the switching frequency allows a reduction of the size of the EMI filter which has to be provided at the input of the rectifier for preventing harmonic interference of other systems operating in parallel.

Remark: The influence of ρ_{--} on the center point current i_M (and on the rms value of the mains current harmonics $\Delta I_{N,\text{rms}}$) will be discussed in detail in section 4 and section 5.1, and therefore will be neglected in the following for the sake of clearness.

3.1 Definition of the Modulation Scheme

In order to obtain a maximum reduction of the switching losses of a bridge leg a switching of the power transistor has to be avoided in the vicinity of the maxima of the associated phase current. This basic idea results (in connection with providing a zero average value of the center point current within a mains period) in a control scheme (a) as described in **Tab.1** for $\frac{1}{3}$ of the mains period. The switching sequences within the sectors of the space vector plane (and/or the intervals of the fundamentals of the mains) which are not described explicitely in Tab.1 can be derived simlpy by a cyclical exchange of the denominations of the phases. As shown in Fig.2 the duration of the clamping of one phase is influenced by the amplitude $\hat{U}_U^*$ and/or the modulation index M. Besides clamping intervals being associated to the turn-off state of a power transistor, there are clamping intervals in the vicinity of the phase current zero-crossings where a transistor remains in the on-state.

In the sectors I and IIa the redundant switching state (011) is used for forming the voltage. This results in the modified switching state sequence as described in Eq.(18) with no switching of phase R. Within sector IIa the power transistor of phase S is switched on. For leaving this sector counterclockwise along a circular trajectory the sign of the phase current $i_{N,S}$ changes, so that according to Eq.(7) the forming of the voltage of the phase S is influenced. For the sectors IIb, III, IV and Va we therefore have a redundancy of the switching states $(s_R, s_S, s_T)_{\text{red}} = (110)$ and (001). If according to control scheme (a) (cf. Tab.1) only the switching state (100) is used incorporated into the switching sequence, the power transistor of phase S will remain in the on-state within sector IIb; furthermore, within the sectors III and IV the power transistor of phase T will be in the off-state, and in sector V the power transistor of phase R will be turned on. Leaving the sector Va makes $i_{N,R}$ negative, correspondingly the redundant switching states of the sectors Vb, VI (and VII and VIIIa) are $(s_R, s_S, s_T)_{red} = (101)$ and (010). Further considerations of the sectors Vb and VI show that in case of an elimination of the switching state (010) in sector Vb phase R will be remain on and in sector VI (also in sector VII if continued) phase S will be remain off. Therefore, one can say that the bridge legs of the system are not switched continuously during one mains period (*continuous modulation*), but are switched discontinuously by clamping the power transistor of one phase in on-state or off-state in the vicinity of the maxima and the zero-crossings of the associated mains currents. Therefore, in analogy to similar control schemes for two-level converters [3], [10] the modulation scheme is denominated as *discontinuous modulation* in the following.

Besides control scheme (a) Tab.1 also details a control scheme (b), which is charactericed by a width of the clamping intervals being independent of the modulation index M and inverse values of ρ_{--} as compared to control scheme (a). Here, the clamping takes place in $\frac{\pi}{6}$-wide intervals that are shifted by $\pm\frac{\pi}{4}$ out of the maxima of the associated mains phase currents; as shown in the following section this results in the region of a high modulation index M (which is of special interest as described in connetion with Eq.(6)) in in a lower reduction of the switching losses as compared to control scheme (a). Therefore, the analysis performed in this paper will be limited to control scheme (a) in the following.

3.2 Reduction of the Switching Losses as Compared to Continuous Modulation

In the following the reduction of the switching losses as compared to a continuous modulation for clamping of one phase and/or the increase of the switching frequency being admissible for equal thermal stress on the valves will be calculated.

As shown in [12] the (global) switching losses of the transistor of a bridge leg can be calculated by averaging the local switching losses $p_T = \frac{1}{T_P} w_P$ according to

$$P_T = \frac{1}{\frac{\pi}{2}} \int_0^{\frac{\pi}{2}} p_T \, \mathrm{d}\varphi_N \, . \tag{19}$$

There, the integration can be limited to $\frac{1}{4}T_N$ or $\frac{\pi}{2}$ due to symmetry reasons. The switching loss, i.e. the sum of the turn-on loss and the turn-off loss) w_P occurring within one pulse period, in correspondence to measurements performed in [12] (cf. Fig.6 in [12]) can be expressed in linear dependency on the switched current

$$w_T = k\, i_N \tag{20}$$

with good approximation. For continuous modulation there follows for the simplifying assumption of a purely sinusoidal shape of the switched current

$$P_{T,(c)} = \frac{2}{\pi} k \hat{I}_N f_P \, . \tag{21}$$

For discontinuous modulation in course of the integration those intervals have to be omitted where the power transistor considered remains in turn-on or turn-off state. If in consequent approximation the phase difference between the reference voltage space vector $\underline{u}_U^*$ (defining the modulation index M) and the space vector $\underline{i}_N^*$ of the mains phase current is neglected, (cf. Eq.(3), $\omega_N L \hat{I}_N^* \approx 0.005 \ldots 0.02 \hat{U}_N$ typically), for modulation scheme (a) the integration is restricted to segments of the trajectory of $\underline{u}_U^*$ lying in the sectors II, III and IV. For modulation scheme (b) only the segments of the trajectory lying in the sectors I, IIa, IV and Va have to be taken into account.

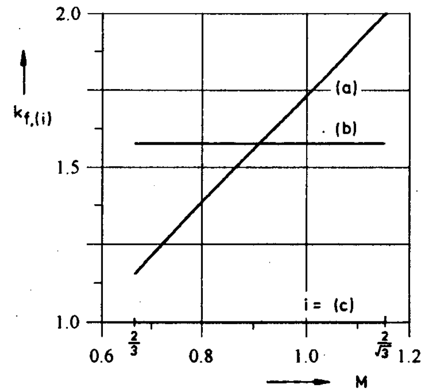

Fig.3: Possible increase k_{f}, i of the effective switching frequency for discontinuous modulation (a) (cf. Eq.(23)) or (b) (cf. Eq.(24)) compared to continuous modulation with switching frequency f_P in dependency of the modulation index M.

Because the integration interval is dependent on the modulation index M the switching losses resulting for modulation scheme (a) also show a dependency on the modulation index M

$$P_{T,(a)} = \frac{2}{\pi} \frac{1}{\sqrt{3}M} k \hat{I}_N f_P \, . \tag{22}$$

Close to the overmodulation limit $M = M_{max}$ the switching losses are reduced with by factor of 2 as compared to continuous modulation, for $M = \frac{2}{3}$ there is a reduction by a factor of $\frac{\sqrt{3}}{2}$. As shown in section 5.2 the conduction losses are in good approximation independent of the modulation scheme (continuous or discontinuous modulation). Therefore, under the assumption of equal thermal stress on the power transistors as compared to continuous modulation (cf. Eq.(21)) the switching frequency of the discontinuous modulation scheme (a) can be increased by a factor of

$$k_{f,(a)} = \frac{1}{\sqrt{3}M} \tag{23}$$

(cf. **Fig.3**). A similar consideration shows for the modulation scheme (b) the possibility of increasing the switching frequency by a factor of

$$k_{f,(b)} = \frac{2}{3 - \sqrt{3}} \approx 1.58 \tag{24}$$

(cf. Fig.3). In contrast to (a) there is no dependency of k_f on M for modulation scheme (b). This can be explained by the independency of the relative duration and position of the clamping intervals of M for scheme (b).

4 RMS Value of the Mains Current Harmonics

As compared to continuous modulation for discontinuous modulation in general a lower ripple of the mains phase current can be expected due to the higher effective switching frequency (cf. Fig.3). Besides the switching frequency the ripple of the mains phase current is also influenced by the distribution ρ_{--} of the redundant switching states between begin and end of one pulse half period. This becomes immediately clear by considering

$$L\frac{d\Delta \underline{i}_N}{dt} = \underline{u}_U^* - \underline{u}_{U,j} \tag{25}$$

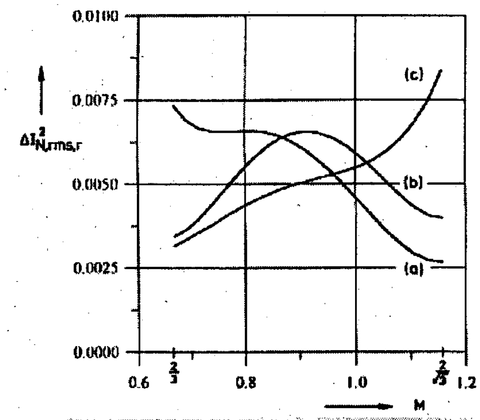

Fig.4: Dependency of the normalized harmonic losses of one phase (the square of the rms value of the phase current ripple) on the modulation index M for discontinuous modulation (a) (cf. (a) and (b) (cf. (b)) and for harmonic-optimal continuous modulation (c) (cf. (c)); for (a) and (b) the possible increase k_f of the switching frequency (dependent on the modulation index M, cf. Fig.3) as compared to the continuous modulation is taken into account.

(cf. Eq.(32) in PESC96[13]). $\Delta \underline{i}_N$ denotes the space vector of the ripple components of the mains phase current. According to Eq.(25) the harmonics with switching frequency of the mains current are caused by the difference between the reference space vector $\underline{u}_U^*$ (which has to be generated for a purely sinusoidal mains current shape) and the space vector $\underline{u}_{U,j}$ (which exists actually in the respective instant). (In case of continuous motion of $\underline{u}_{U,j}$ along a circular trajectory $\underline{u}_U^*$ and/or purely sinusoidal rectifier input voltages $u_{U,i}$ the mains current would be purely sinusoidal which is equivalent to $\Delta \underline{i}_N = 0$). Therefore, a change of the distribution ρ_{--} of the redundant switching states directly influences the shape of the trajectory of $\Delta \underline{i}_N$ and results in a change of the rms value of the mains current harmonics.

As a detailed analysis (which has to be omitted here for the sake of brevity) shows [14], the rms value of the mains current ripple can be minimized for continuous modulation by defining $\rho_{--} \approx 0.5$ in wide intervals of the mains period. Therefore, for discontinuous modulation being characterized by $\rho_{--} = 0$ or 1 (cf. Tab.1) a harmonic-optimal operation cannot be expected. The reduction of the ripple via increasing the switching frequency by a factor $k_{f,(i)}$ is partly offset by the not optimal distribution of the redundant switching states. The resulting characteristics of the harmonics of the mains current are shown for discontinuous modulation (a) and (b) and harmonic-optimal continuous modulation (c) in **Fig.4**. For discontinuous modulation (a) the analytical calculations

$$\Delta I^2_{N,rms,r} = \frac{1}{3M^2}\Big[\frac{20}{9} + \frac{2}{\pi}\big(\sqrt{3} - \frac{28}{9}\arcsin(\frac{1}{\sqrt{3}M})\big) + M^2\big(13 + \frac{5\sqrt{3}}{\pi} - \frac{34}{\pi}\arcsin(\frac{1}{\sqrt{3}M})\big) + \frac{3}{2}M^4\big(1 + \frac{3\sqrt{3}}{2\pi}\big) - \frac{308}{9\sqrt{3}\pi}M\sqrt{1 - \frac{1}{3M^2}} - \frac{2}{3\sqrt{3}\pi}M^3\big(4 + 83\sqrt{1 - \frac{1}{3M^2}}\big)\Big] . \tag{26}$$

show a very good correspondence with the results of the digital simulation.

Time behavior and amplitude spectrum of the ripple $\Delta i_{N,R}$ of the mains current of modulation schemes (a) and (c) are shown in **Fig.5** for $M = 1.085$ according to an output voltage $U_O = 600\,V$ for $U_{N,rms} = 230\,V$

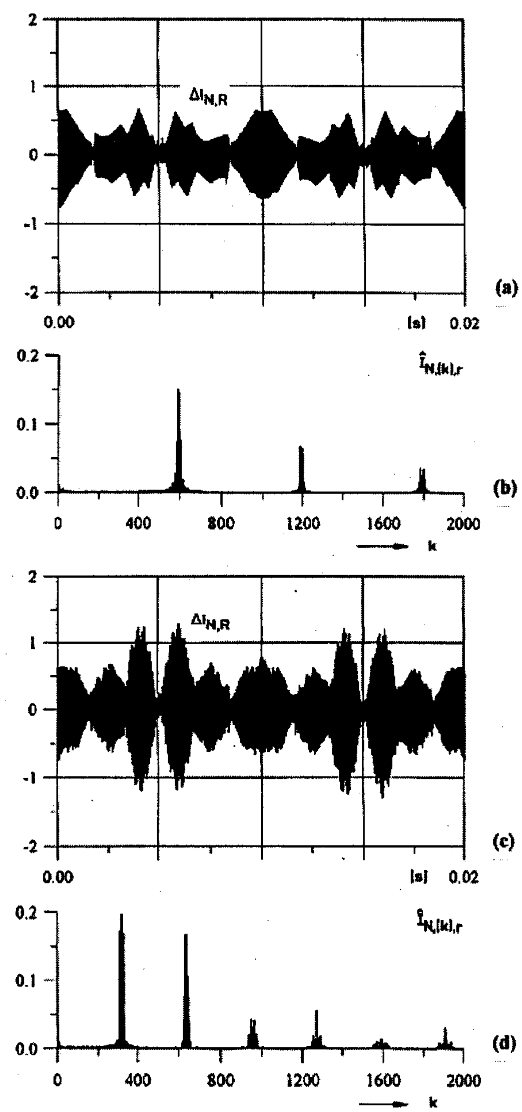

Fig.5: Time behaviour (1 A/div) and amplitude spectrum (amplitudes of the harmonics normalized to the fundamental $\hat{I}_{N,(1)}$ of the mains phase current, harmonic order k referring to the mains frequency f_N) of the phase current ripple $\Delta i_{N,R}$ for discontinuous modulation (a) (cf. (a), $f_P = 29.9\,$kHz) and harmonic-optimal continuous modulation (c) (cf. (c), $f_P = 16\,$kHz); $M = 1.085$ and/or $U_O = 600\,$V, other simulation parameters according to the values in section 2.2.

Operating the rectifier close to the overmodulation limit in case of modulation scheme (a) reduces the harmonic losses by a factor of ≈ 3 as compared to optimized conthe distribution ρ_{--} of the redundant switching states between begin and end of one pulse half period. This becomes immediately clear by considering

$$L\frac{\mathrm{d}\Delta\underline{i}_N}{\mathrm{d}t} = \underline{u}_U^* - \underline{u}_{U,j} \tag{25}$$

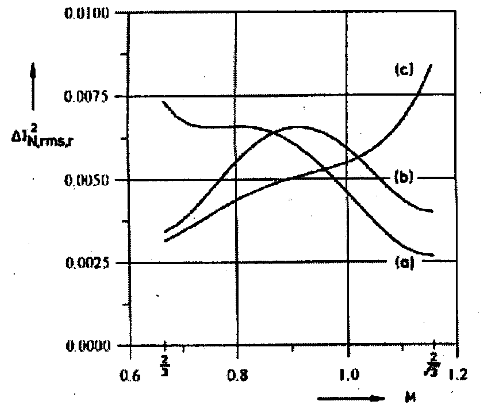

Fig.4: Dependency of the normalized harmonic losses of one phase (the square of the rms value of the phase current ripple) on the modulation index M for discontinuous modulation (a) (cf. (a) and (b) (cf. (b)) and for harmonic-optimal continuous modulation (c) (cf. (c)); for (a) and (b) the possible increase k_f of the switching frequency (dependent on the modulation index M, cf. Fig.3) as compared to the continuous modulation is taken into account.

(cf. Eq.(32) in PESC96[13]). $\Delta\underline{i}_N$ denotes the space vector of the ripple components of the mains phase current. According to Eq.(25) the harmonics with switching frequency of the mains current are caused by the difference between the reference space vector $\underline{u}_U^*$ (which has to be generated for a purely sinusoidal mains current shape) and the space vector $\underline{u}_{U,j}$ (which exists actually in the respective instant). (In case of continuous motion of $\underline{u}_{U,j}$ along a circular trajectory $\underline{u}_U^*$ and/or purely sinusoidal rectifier input voltages $u_{U,i}$ the mains current would be purely sinusoidal which is equivalent to $\Delta\underline{i}_N = 0$). Therefore, a change of the distribution ρ_{--} of the redundant switching states directly influences the shape of the trajectory of $\Delta\underline{i}_N$ and results in a change of the rms value of the mains current harmonics.

As a detailed analysis (which has to be omitted here for the sake of brevity) shows [14], the rms value of the mains current ripple can be minimized for continuous modulation by defining $\rho_{--} \approx 0.5$ in wide intervals of the mains period. Therefore, for discontinuous modulation being characterized by $\rho_{--} = 0$ or 1 (cf. Tab.1) a harmonic-optimal operation cannot be expected. The reduction of the ripple via increasing the switching frequency by a factor $k_{f,(i)}$ is partly offset by the not optimal distribution of the redundant switching states. The resulting characteristics of the harmonics of the mains current are shown for discontinuous modulation (a) and (b) and harmonic-optimal continuous modulation (c) in **Fig.4**. For discontinuous modulation (a) the analytical calculations

$$\Delta I^2_{N,rms,r} = \frac{1}{3M^2}\Big[\frac{20}{9} + \frac{2}{\pi}(\sqrt{3} - \frac{28}{9}\arcsin(\frac{1}{\sqrt{3}M})) + M^2(13 + \frac{5\sqrt{3}}{\pi} - \frac{34}{\pi}\arcsin(\frac{1}{\sqrt{3}M})) + \frac{3}{2}M^4(1 + \frac{3\sqrt{3}}{2\pi}) - \frac{308}{9\sqrt{3}\pi}M\sqrt{1-\frac{1}{3M^2}} - \frac{2}{3\sqrt{3}\pi}M^3(4 + 83\sqrt{1-\frac{1}{3M^2}})\Big]\,. \tag{26}$$

show a very good correspondence with the results of the digital simulation.

Time behavior and amplitude spectrum of the ripple $\Delta i_{N,R}$ of the mains current of modulation schemes (a) and (c) are shown in **Fig.5** for $M = 1.085$ according to an output voltage $U_O = 600\,V$ for $U_{N,rms} = 230\,V$

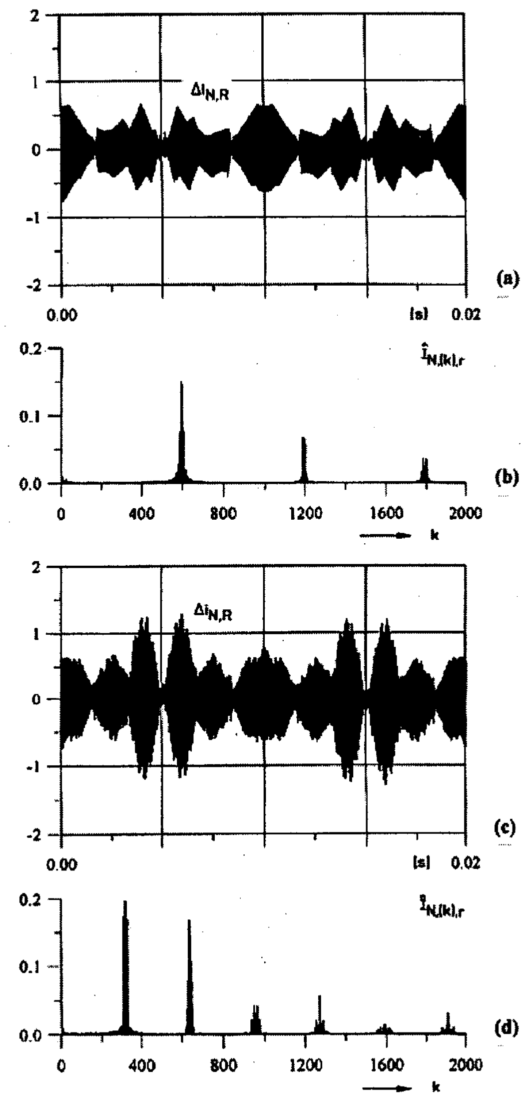

Fig.5: Time behaviour (1 A/div) and amplitude spectrum (amplitudes of the harmonics normalized to the fundamental $\hat{I}_{N,(1)}$ of the mains phase current, harmonic order k referring to the mains frequency f_N) of the phase current ripple $\Delta i_{N,R}$ for discontinuous modulation (a) (cf. (a), f_P = 29.9 kHz) and harmonic-optimal continuous modulation (c) (cf. (c), f_P = 16 kHz); $M = 1.085$ and/or $U_O = 600\,$V, other simulation parameters according to the values in section 2.2.

Operating the rectifier close to the overmodulation limit in case of modulation scheme (a) reduces the harmonic losses by a factor of ≈ 3 as compared to optimized continuous modulation (c) (the rms value of the mains current harmonics is then reduced by a factor of $\sqrt{3}$). Employing modulation scheme (b) results in reduction of the switching losses by a factor of 2 (the rms value of the mains current harmonics is then reduced by a factor of $\sqrt{2}$). For practical realization, therefore, modulation scheme (a) has to be preferred to scheme (b) although the realization effort for (a) is higher due to the dependency of the clamping intervals on the modulation index M.

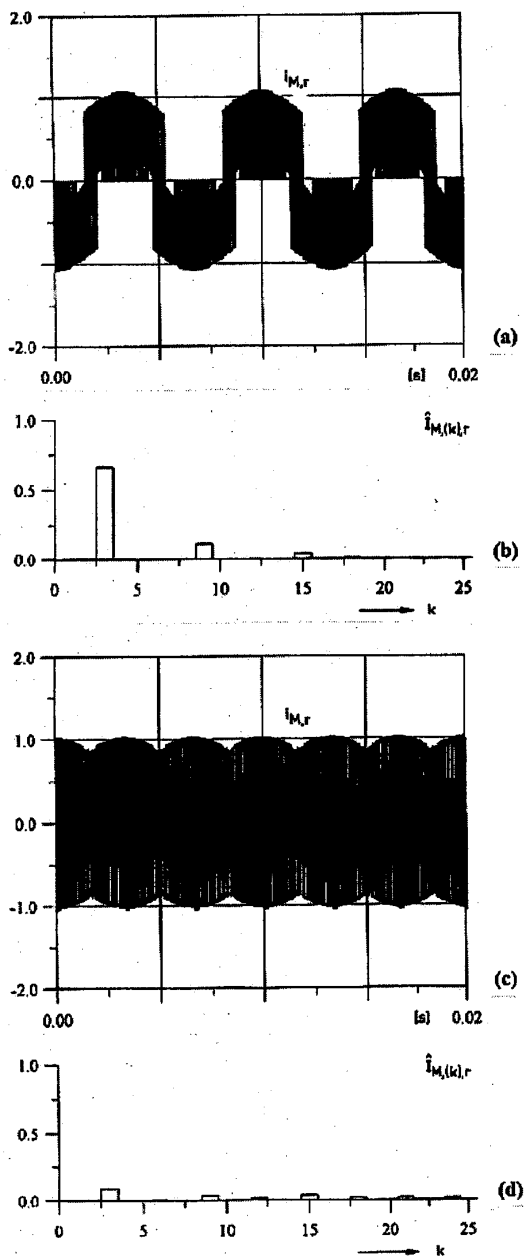

Fig.6: Time behaviour and amplitude spectrum of the normalized (related to the amplitude $\hat{I}_N^*$ of the mains phase current fundamental) center point current i_M for discontinuous modulation (a) (cf. **(a)** and **(b)**) and optimized continuous modulation (c) (cf. **(c)** and **(d)**); k describes the order of the harmonics referring to the mains frequency f_N.

5 Current Stress on the Power Components

According to Eq.(11) and/or Eq.(13) the control parameter ρ_{--} influences not only the harmonics of the mains currents with switching frequency but also takes influence on forming of the center point current i_M. To give a comprehensive analysis of the rectifier system, in the following the stresses on the output capacitors and on the power semiconductors for discontinuous modulation will be compared to harmonic-optimal continuous modulation.

5.1 Output Capacitors

5.1.1 Low-Frequency Harmonics of the Center Point Current and the Output Capacitors

According to the analysis given in section 2.1 (cf. Eq.(13) and Eq.(14)) the maximum negative and/or the maximum positve local average value $i_{M,avg}$ of the center point current occurs during one pulse period for $\rho_{--} = 0$ and/or $\rho_{--} = 1$. The switching of ρ_{--} between 0 and 1 with three times the mains frequency (cf. Tab.1), which is characteristic for discontinuous modulation, therefore, results in a relatively high amplitude of the third harmonic of the center point current (cf. **Fig.6**(a) and (b)). In contrast, for optimized continuous modulation (characterized by $\rho_{--} \approx 0.5$) there is about a compensation of the positive and negative portion of i_M within one pulse period. Therefore, the low-frequency harmonics $\hat{I}_{M,(k)}$ ($k = 3, 9, 15 \ldots$) of i_M show relatively low amplitudes. In order to limit the potential shift of the center point (caused by the harmonics $\hat{I}_{M,(k)}$ of the center point current) to a given maximum value, for discontinuous modulation a higher capacitance of the output capacitors has to be provided.

As shown in **Fig.7** for discontinuous modulation (a) with increasing modulation index M there is an approximately linear decline of the amplitude of the third harmonic of the center point current. This can be explained by the declining sum of the duration of the redundant switching states, which is also linear with M and which results in a proportional reduction of the local average value and amplitude of the low-frequency harmonics of the center point current. For a high modulation index the base for calculating the necessary output capacitance is therefore (using electrolyt capacitors) not the above described potential shift of the center point but the rms value of the capacitor current which will be calculated in the following.

5.1.2 RMS Value of the Output Capacitor Current

In contrast to the low-frequency harmonics of i_M the rms value of the output capacitor current is *not* influenced by the control parameter ρ_{--} and can, therefore, be calculated for (optimized) continuous modulation and discontinuous modulation as

$$I^2_{C,rms,r} = \frac{10\sqrt{3}M}{8\pi} - \frac{9M^2}{16}\,. \tag{27}$$

For the redundant switching states the center point current shows different signs but equal absolute value (cf. Eq.(11). Therefore, the rms value of the current being fed into the capacitive center point M and being distributed between the both output capacitors equally and/or the output capacitor rms value are independent of ρ_{--}. A more detailed analysis of this fact can be found in [14].

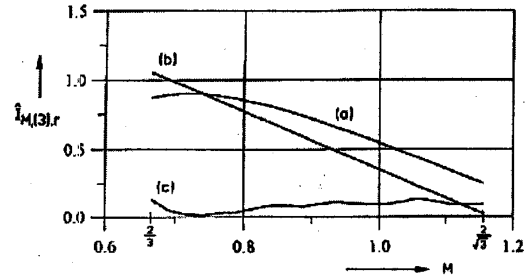

Fig.7: Dependency of the normalized amplitude $\hat{I}_{M,(3),r}$ of the third harmonic of the center point current on the modulation index M for discontinuous modulation (a) and (b) (cf. (**a**) and (**b**)) and optimized continuous modulation (c) (cf. (**c**)).

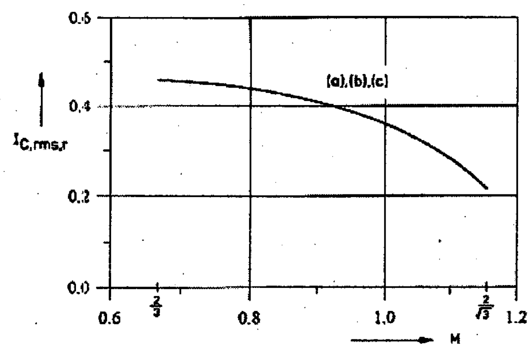

Fig.8: Normalized rms value $I_{C,rms,r} = I_{C+,rms,r} = I_{C-,rms,r}$ of the output capacitor currents i_{C_+} and i_{C_-} in dependency on the modulation index M. The current stress on C_+ and C_- is not influenced by the modulation scheme (by the control parameter ρ_{--}).

5.2 Power Semiconductors

As a detailed analysis shows, the current stress on the power semiconductors (average and rms value) is only marginally influenced (divergence smaller than 5%) by a transition from continuous to discontinuous modulation. For the average values of the currents of the devices this can be checked easily, as shown in the following. A detailed analytical calculation of the rms values of the currents is more complicated and will be omitted here for the sake of brevity.

According to

$$I_{+,avg} = I_{-,avg} = I_O = \frac{P_O}{U_O} \qquad P_O = \frac{3}{2}\hat{U}_N \hat{I}_N \quad (28)$$

the average current $I_{+,avg}$ and/or $I_{-,avg}$ in the positive and/or negative output voltage bus for a given output voltage U_O is coupled directly to the output power P_O and/or the amplitude $\hat{I}_N = \hat{I}_{N,(1)}$ of the approximately purely sinusoidal mains current. Therefore, under consideration of the phase-symmetrical topology of the system also the average value $I_{D_F,avg}$ of the current of the free-wheeling diodes D_{F+} and D_{F-}

$$I_{D_F,avg} = \frac{1}{3} I_O = \frac{1}{4} M \hat{I}_N \,. \quad (29)$$

is independent of the actual modulation scheme employed. Because the (approximately sinusoidal) current via the mains side diodes D_{N+} and D_{N-} is not influenced by the switching of the power transistors, we further can write independently of the modulation scheme

$$I_{D_N,avg} = \frac{1}{\pi}\hat{I}_N \,. \quad (30)$$

For the average value of the current through the power transistor there follows directly

$$I_{T,avg} = 2(I_{D_N,avg} - I_{D_F,avg}) = 2(\frac{1}{\pi} - \frac{M}{4})\hat{I}_N \quad (31)$$

where a factor of 2 has to be considered (in contrast to the diodes $D_N i$ and $D_F i$, $i = +,-$) because the power transistor T carries current within the positive *and* the negative mains half period. With Eq.(31) there directly follows for the average value of the center point diode current as

$$I_{D_M,avg} = \frac{1}{2} I_{T,avg} . \quad (32)$$

In summary, the average values of the currents of all power semiconductors are not influenced by the control parameter ρ_{--} and can be calculated directly based on the mains current amplitude $\hat{I}_N$ for a given modulation index M.

For the rms value of the power transistor current a more complex analytical calculation results in

$$I^2_{T,rms} = \frac{1}{2\pi}\Big[\frac{5\pi}{3} - \sqrt{3} + \frac{1}{4\sqrt{3}M^3}(1+\frac{5M}{3}) - 2\arcsin(\frac{1}{\sqrt{3}M}) - \frac{4}{\sqrt{3}}(M+\frac{1}{6M})\sqrt{1-\frac{1}{3M^2}}\Big]\hat{I}^2_N \,. \quad (33)$$

As a comparison with the result of an analogous calculation for harmonic-optimal continuous modulation confirms, the control parameter ρ_{--} takes only low influence on the current stress (rms value) on the power transistors. The rms value of the current of the mains side diodes D_N can be calculated directly via

$$I_{D_N,rms} = \frac{1}{2}\hat{I}_N \,. \quad (34)$$

For the currents $I_{D_F,rms}$ and $I_{D_M,rms}$ we obtain therefore

$$I^2_{D_F,rms} = I^2_{D_N,rms} - \frac{1}{2}I^2_{T,rms} \qquad I^2_{D_M,rms} = \frac{1}{2}I^2_{T,rms} \,. \quad (35)$$

In summary, the use of continuous or discontinuous modulation primarily effects the switching losses, the conduction losses according to the average and rms values of the currents through the devices are not influenced in a first approximation. This confirms the assumption (made by turning Eq.(23) into Eq.(24)) that for discontinuous modulation the possible increase k_f of the switching frequency f_P is only defined by the switching losses.

6 Modulation Functions

In the previous sections the switching sequence and/or the control parameter ρ_{--} was used to define the discontinuous modulation. This relatively abstract analysis based on space vector calculus gives a clear description of the operating principle of the rectifier system. But for a more illustrative description, e.g. of the clamping of the single switching frequency of the system can be increased or the rms value of the mains current ripple can be reduced for equal rated power of the input inductors L. (Changing from continuous modulation to discontinuous modulation only takes marginal influence on the current average and rms values and/or on the conduction losses of the power semiconductors.) However, these advantages are only given for high modulation index. For rectifier systems of high power and/or low switching frequency discontinuous modulation can be used to increase the effective switching frequency above the audible range in order to avoid annoying noise during operation. Alternatively, it is possible to increase the system efficiency due to reduced switching losses for equal rms value of the mains current ripple as compared to a system using continuous modulation. (The switching frequency is in this case still higher than in case of continuous modulation.) As disadvantage of discontinuous modulation one has to mention the relatively high amplitudes of the low-frequency harmonics of the center point current which result in the requirement of a higher output capacitance for a given admissinble voltage ripple of the center point potential. Another disadvantage is the higher complexity of the control of the center point potential.

Finally we want to point out that concerning the mains current harmonics with switching frequency the main advantage of discontinuous modulation as compared to continuous modulation is the possibility of increasing the effective switching frequency (and not primarily the reduction of the rms value of the mains current ripple). If for comparing the modulation schemes the EMI-filter (which has to be provided in any case at the input side of the rectifier for a practical realization) is taken into accout, for a second order filter with a cut-off frequency being considerably lower than the switching frequency doubling of the switching frequency will result in an increase of the attenuation by a factor of 4. This increase in attenuation is by far more effective than the reduction of the rms value of the mains current ripple due to the increase of the effective switching frequency (factor $\approx \sqrt{3}$, cf. Fig.4). If the rms value of the mains current ripple is thought to be concentrated in a single harmonic with effective switching frequency, the total improvement of the damping of mains current harmonics caused by discontinuous modulation results to a factor of $\approx 4.\sqrt{3} \approx 7$. Therefore, for practical realization of the VIENNA Rectifier one in any case should prefer discontinuous modulation to continuous modulation, especially if high power density and/or low filtering effort and/or small size of the passive components are required.

ACKNOWLEDGEMENT

The authors are very much indebted to the Jubiläumsfonds der OESTERREICHISCHEN NATIONALBANK which generously supports the work of the Department of Electrical Drives and Machines of the Technical University of Vienna.

References

[1] **Mohan, N., Undeland, T. M., and Robbins, W. P.:** *Power Electronics: Converters, Applications and Design.* 2nd Edition, New York: John Wiley & Sons (1995).

[2] **Depenbrock, M:** *Pulse Width Control of a 3-Phase Inverter with Non-Sinusoidal Phase Voltages.* Proceedings of the International Semiconductor Power Converter Conference, Orlando, FL, March 28–31, pp. 399–403 (1977).

[3] **Kolar, J. W., Ertl, H., and Zach, F. C.:** *Influence of the Modulation Method on the Conduction and Switching Losses of a PWM Converter System.* Conference Record of the 25th IEEE Industry Applications Society Annual Meeting, Seattle, WA, Oct. 7–12, Pt. 1, pp. 502–512 (1990). Also published in: IEEE Transaction on Industry Applications, Vol. IA-37, No. 6, pp. 1063–1075 (1991).

[4] **Kolar, J. W., and Zach, F. C.:** *A Novel Three-Phase Three-Switch Three-Level PWM Rectifier.* Proceedings of the 28th Power Conversion Conference, Nürnberg, Germany, June 28–30, pp. 125–138 (1994).

[5] **Koczara, W., and Bialoskorski, P.:** *Multilevel Boost Rectifiers as a Unity Power Factor Supply for Power Electronics Drive and for Battery Charger.* Conference Proceedings of the IEEE International Symposium on Industrial Electronics, Budapest, June 1–3, pp. 477–481 (1993).

[6] **Zhao, Y., Li, Y., and Lipo, T. A.:** *Force Commutated Three-Level Boost Type Rectifier.* Conference Record of the 28th IEEE Industry Applications Society Annual Meeting, Toronto, Oct. 2–8, Pt. II, pp. 771–777 (1993).

[7] **Kolar, J. W., and Zach, F. C.:** *A Novel Three-Phase Utility Interface Minimizing Line Current Harmonics of High-Power Telecommunications Rectifier Modules.* Record of the 16th IEEE International Telecommunications Energy Conference, Vancouver, Canada, Oct. 30–Nov. 3, pp. 367–374 (1994).

[8] **Fukuda, S., and Sagawa, A.:** *Modelling and Control of a Neutral-Point-Clamped Voltage Source Converter.* Proceedings of the International Power Electronics Conference, Yokohama, Japan, April 3–7, Vol. 1, pp. 470–475 (1995).

[9] **Kolar, J.W., Drofenik, U., and Zach, F.C.:** *Space Vector Based Analysis of the Variation and Control of the Neutral Point Potential of Hysteresis Current Controlled Three-Phase/Switch/Level PWM Rectifier Systems.* Proceedings of the International Conference on Power Electronics and Drive Systems, Singapore, Feb. 21–24, Vol.1, pp. 22–33 (1995).

[10] **Holtz, J.:** *Pulsewidth Modulation – A Survey.* IEEE Transactions on Industrial Electronics, Vol. 39, No. 5, pp. 410–420 (1992).

[11] **Kolar, J.W., Drofenik, U., and Zach, F.C.:** *DC Link Voltage Balancing of Three-Phase/Switch/Level PWM (VIENNA) Rectifier by Modified Hysteresis Input Current Control.* Proceedings of the 30th International Power Conversion Conference, Nürnberg, Germany, June 20–22, pp. 443–465 (1995).

[12] **Kolar, J.W., Ertl, H., and Zach F.C.:** *Design and Experimental Investigation of a Three-Phase High Power Density High Efficiency Unity Power Factor PWM (VIENNA) Rectifier Employing a Novel Power Semiconductor Module.* Proceedings of the 11th IEEE Applied Power Electronics Conference, San Jose (CA), March 3–7, Vol. 2, pp. 514–523 (1996).

[13] **Kolar, J.W., Drofenik, U., and Zach, F.C.:** *Current Handling Capability of the Neutral Point of a Three-Phase/Switch/Level Boost-Type PWM (VIENNA) Rectifier.* Proceedings of the 27th IEEE Power Electronics Specialists Conference, Baveno, Italy, June 24–27, Vol. II, pp. 1329–1336 (1996).

[14] **Kolar, J. W., Drofenik, U., and Zach, F. C.:** *AC- or DC-Side Optimum Stationary Operation of a High-Frequency Unidirectional Three-Phase Three-Switch Neutral Point Clamped PWM Rectifier.* Currently under review for publication at the 7th International Power Electronics and Motion Control Conference, Budapest, Sept. 2–4 (1996).

[15] **Shimane, K., and Nakazawa, Y.:** *Harmonics Reduction for NPC Converter with a New PWM Scheme.* Proceedings of the International Power Electronics Conference, Yokohama, Japan, April 3–7, Vol. 1, pp. 482–487 (1995).